

# TESTS AND MEASUREMENTS WITH THE EMBEDDED RADIATION-MONITOR-SYSTEM PROTOTYPE FOR DOSIMETRY AT THE EUROPEAN XFEL

Frank Schmidt-Foehre, Dirk Noelle, Rainer Susen, Kay Wittenburg, DESY, Hamburg

## Abstract

A new Embedded Radiation-Monitor-System is under development for the European XFEL (E-XFEL), that is being built between the DESY campus at Hamburg and Schenefeld at Schleswig-Holstein [1,2].

Most of the electronic systems cabinets for machine control, diagnostics and safety of the E-XFEL will be located in cabinets inside the accelerator tunnel. All electronic cabinets inside the tunnel will be sufficiently shielded according to pre-estimated radiation levels to prevent significant radiation damage at electronic systems in certain sections of the E-XFEL. In addition, the accumulated dose inside these cabinets will be monitored for the impact of Gamma- and Neutron-radiation by a new radiation monitor system [3]. This system will also be used to monitor the dose rates in the undulator regions. Lifecycle estimations for the electronics and undulators define radiation damage thresholds. In time part exchange is foreseen before significant radiation damage occurs.

The prototype of the Gamma radiation-monitor system section has been successfully designed and tested at the DESY Linac II using a RadFet-type [4] RFT-300-CC10G1 sensor chip (REM Oxford Ltd., [5]). Prototype tests and according measurements will be presented.

## INTRODUCTION

The E-XFEL will be able to deliver photons to several user stations simultaneously, utilizing different spontaneous and Free-Electron Laser sources. High average and peak brilliance can be produced based on superconducting technology, providing electron beams with high duty cycles. An acceleration up to 17.5 GeV at RF repetition rates of 10 Hz (higher rep rates available at lower gradients) can be applied to bunches with repetition rates up to 4.5 MHz at macro pulse lengths up to 600  $\mu$ s. Flexible bunch patterns will offer optimum tuning to the experiments demands [6].

The highest dose rates of parasitic radiation seen by the electronic racks and undulators in the tunnel are expected during accelerator commissioning or inadvertent mis-operation at later operational phases. Rates up to 8 Gy for  $\gamma$ -dose and  $5.6 \times 10^{10}$  cm<sup>-2</sup> of neutron fluence over 10 years inside the sufficiently shielded E-XFEL frontend-electronic racks were estimated [7]. Measurements at the FLASH FEL (2005-2008) [8] resulted in a worst-case scenario of up to 2 kGy/a, expecting a theoretical 10-years-accumulated  $\gamma$ -dose of  $\approx$  20 kGy as a radiation damage threshold of the undulators. The  $\gamma$ -radiation measurement of the new radiation monitor testboard (TB) prototype is designed to cope with these radiation levels. An irradiation test-stand has been set up at the DESY

Linac II converter for prototype tests and measurements with the new electronics, which are presented below.

## TEST SETUP AT IRRADIATION SOURCE

High parasitic radiation fields are generated in the Linac II electron/positron converter by the accompanying electromagnetic shower. A fast and easily removable probe plate (carrier) has been located in a high irradiation area below the converter. As confirmed by simulation, the received dose rate levels are uniformly distributed over the plate area. The carrier offers four test sensor positions, ensuring equal dose rates at each position pair. A central position on the carrier plate aligned with the vertical beam plane is able to hold other, easily removable radiation sensors for reference and calibration measurements. Thermo-Luminescence-Dosimeters (TLD) type TLD-100 are used as a dose-reference for tests at low to medium dose levels up to 3 kGy, whereas TLD-800 serve for high dose measurements up to 10-15kGy [9].

Fig. 1 shows the corresponding energy spectrum estimation in the region of the carrier. Absolute dose levels shown in Fig. 1 are over-estimated due to the simplified geometric model used. In principle, Neutron levels are shown to be more than two orders of magnitude below the  $\gamma$ -radiation level and the TLD reference sensors used are sensible to the main part of the energy distribution [9].

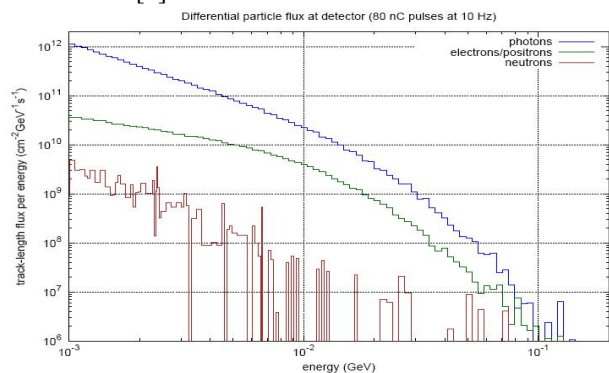


Figure 1: Simulated radiation energy spectrum near the test-stand plate at the DESY LINAC II converter (FLUKA 2011[10, 11]).

## CROSS CALIBRATION

The RadFet-voltage response diagram of a 15-days long-term comparison test between pre-calibrated readout electronics (called Fermi-reader, FR [12]) developed for Fermi@Elettra at Trieste/Italy and the TB is shown in Fig. 2. As a consequence of radiation-induced errors in the network-interface of the FR, the device frequently suspended operation (missing parts of upper curve). With

the exception of the strongly different readout-timing duty-cycles at both curves, resulting in a comparatively lower sensitivity of the TB that is probably caused by reduced RadFet sensitivity during the short readout phase, both curves show good synchronism with non-linear, correctable dependence.

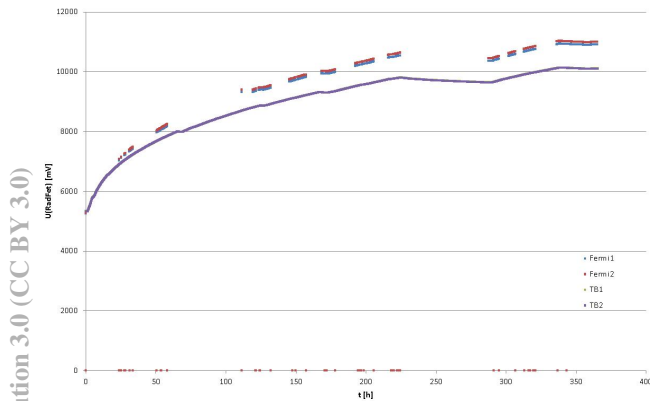


Figure 2: Irradiation test ‘Testboard- vs Fermi-reader’ for cross-calibration at high dynamic dose range.

Fig. 3 shows the impact of RadFet (RF) readout timing at irradiation test over a medium dose range. The lower curve corresponds to frequent readout cycle mode (3s cycle at RF A.51), while the upper 3 curves depict the response on the same radiation with a 54s readout cycle timing (FR-compatible). A remaining difference between the results from Fig. 2 and Fig. 3 is currently under investigation.

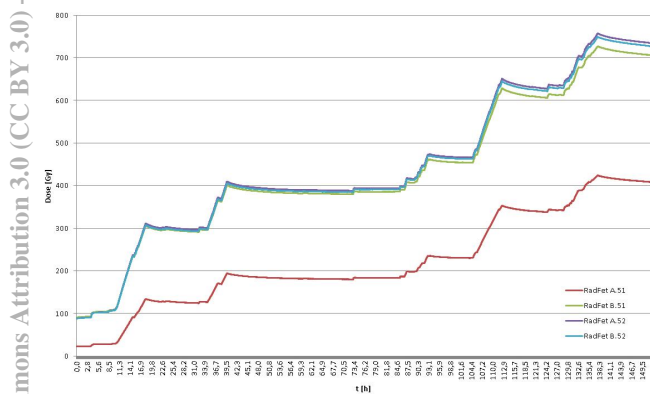


Figure 3: Impact of RadFet readout timing at irradiation test over medium dose range (RF A.51: 3s; other: 54s).

**TEMPERATURE TESTS AND LOGGING**

Fig. 4 shows temperature impacts on the threshold voltage of pre-irradiated RadFets at different dose levels and temperatures. Heavy fading of radiation-induced, trapped charges [4] was observed at higher temperatures together with the semiconductor-induced temperature voltage shift showing a negative temperature-coefficient. In other TB measurements, fading of constant pre-irradiation dose level of up to 15% per month was observed even at room temperature.

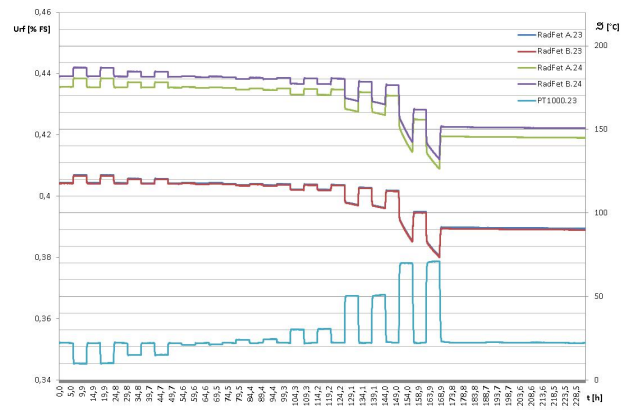


Figure 4: Temperature impacts on threshold voltage of pre-irradiated RadFets at different dose levels (RF23: ~2.5kGy; RF24: ~4kGy).

The TB design also incorporates temperature logging capabilities, using different temperature sensors. Fig. 5 shows a comparison of the radiation-performance of different temperature sensors at a cumulative  $\gamma$ -end-dose of approx. 1.5kGy.

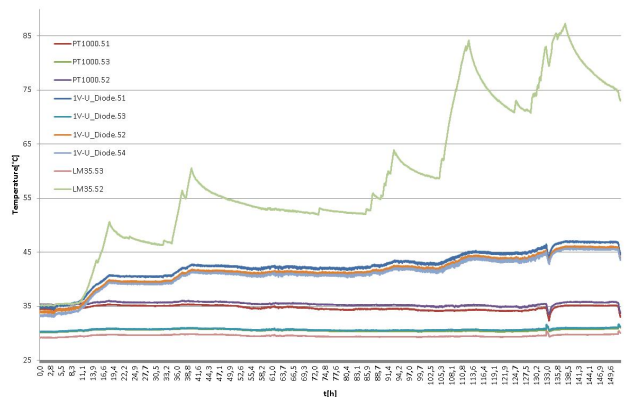


Figure 5: Radiation-performance comparison of different temperature sensors (cumulative  $\gamma$ -dose ~1.5kGy).

The upper curve shows heavily irreversible degrading of the corresponding LM35 chip. Comprehensive tests of several sensor types (LM35, KTY.81, PT1000) showed, that the PT1000 worked without significant degradation in long-term irradiation tests even at high dose levels above 10kGy. The 3 curves below the upper curve (LM35.52) show a slight degradation of the temperature-logging-diodes on the RadFet chips. Investigations on a correction scheme for these diodes are underway.

**POSITIONS AND OPERATIONAL MODES**

The tests have shown sufficient sensitivity and dynamic dose range of the selected RadFet  $\gamma$ -sensors for its locations near the beam pipe (e. g. at undulator positions with up to 2kGy/a estimated dose rate). Nevertheless a significantly higher sensitivity of the sensors is needed for sensor positions inside the electronic racks along the E-XFEL. Fig. 6 shows RadFet threshold

Copyright © 2012 by IEEE - cc Creative Commons Attribution 3.0 (CC BY 3.0) — cc Creative Commons Attribution 3.0 (CC BY 3.0)

voltage (= readout voltage – unirradiated offset-voltage) response at different dose rates using different operational modes of the RadFet sensors. The lowest curves were taken in the RadFet positive bias mode [4] and show a significantly higher sensitivity up to a dose of  $\approx 5\text{Gy}$ . The remaining curves show responses of simultaneously irradiated RadFets at medium dose levels of up to  $\approx 1.5\text{kGy}$ . The upper curve shows performance at a bias of  $-12\text{V}$ , resulting in an increased sensitivity compared to the non-bias standard readout mode (single dark-red curve (RF A.51) in the middle of the diagram).

Analysis of the usability of bias-modes in respect to E-XFEL operation modes is currently under investigation.

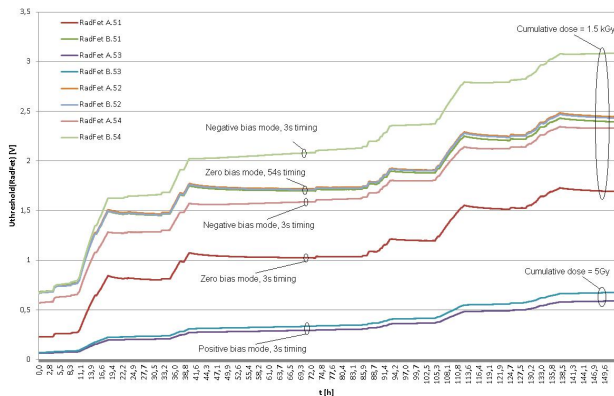


Figure 6: RadFet response due to different RadFet operational modes under irradiation at DESY LINAC II converter.

### CONCLUSION AND OUTLOOK

The performance of the new readout-electronics for the RadFet  $\gamma$ -sensors for the E-XFEL dosimetry system has been investigated. First  $\gamma$ -measurements at the DESY Linac II converter showed, that the principle of the RadFet sensor and its readout system works successfully. A cross-calibration approach in reference to the pre-calibrated RadFet-reader used at Fermi accelerator at Elettra (Trieste, Italy) has shown reasonable, comparable results. Remaining discrepancies between the readout of the two different devices are currently under investigation. First measurements have shown significant impacts of other, currently uncorrected parameters, mainly temperature and fading [4]. The existing temperature readout circuits were improved, based on the presented measurements for temperature and irradiation performance. First tests have also shown important aspects of different operational modes for the sensor readout (unbiased, pos. bias, neg. bias), which will be further evaluated and tested for mode selection of both, the high-sensitivity application inside the E-XFEL electronic racks and undulator dosimetry with a high dynamic dose range (0-20kGy).

Ongoing redesign will take care of the correction of temperature effects using the existing temperature reference measurement circuitry inside the TB. In addition, a fading correction algorithm has been worked out and is currently implemented and tested.

Further tests were planned and initiated for direct calibration measurements at external reference sources, cross-calibration at other accelerators and statistics improvement. Additional tests and measurements are planned with the newly developed n-sensor readout system part (n-TB) to be started in summer 2012.

Design iteration towards a pre-series sensor readout-module for combined  $\gamma$ - and n-monitoring system parts was started based on the FMC-standard [13] and is planned for production in early 2013.

### ACKNOWLEDGEMENTS

We thank W. Decking, E. Negodin, J. Herrmann, I. Peperkorn and M. Salmani for fruitful discussions and L. Fröhlich for his substantial support and many valuable discussions on RadFet related aspects.

### REFERENCES

- [1] M. Altarelli et al., "The European X-Ray Free-Electron Laser", Technical design report, <http://www.xfel.eu/en/documents/>, (2007).
- [2] R. Brinkmann, "The European XFEL Project", FEL'06, Berlin, MOBAU03, p. 24, (2006), <http://www.JACoW.org>
- [3] F. Schmidt-Föhre et. al., „A New Embedded Radiation Monitor System for Dosimetry at the European XFEL”, Proceedings of IPAC11, San Sebastian, Spain, p. 2364 (2011).
- [4] Ravotti et. al., "Development and Characterisation of Radiation Monitoring Sensors for the High Energy Physics Experiments of the CERN LHC Accelerator", CERN-THESIS-2007-013, Genf (2007)
- [5] REM Oxford Ltd., "data sheet RFTDAT-CC10(REV B)", component data sheet rft0888CC10dat0B.doc, Sept 2009, (2009).
- [6] D. Nölle, "Overview on E-XFEL Standard Electron Beam Diagnostics", DESY internal document, (2010)
- [7] E. Negodin, private communication (2009-2011).
- [8] J. Skupin et. al., "Undulator demagnetization due to radiation losses at FLASH", Proceedings of EPAC08, Genoa, Italy, p. 2308 (2008).
- [9] M. Salmani, private communication (2010-2012).
- [10] G. Battistoni et. al., "The FLUKA code: Description and benchmarking", Proceedings of the Hadronic Shower Simulation Workshop 2006, Fermilab 6--8 September 2006, M. Albrow, R. Raja eds., AIP Conference Proceeding 896, 31-49, (2007).
- [11] A. Fasso et. al., "FLUKA: a multi-particle transport code", CERN-2005-10 (2005), INFN/TC\_05/11, SLAC-R-773.
- [12] L. Fröhlich et. al., "Instrumentation for Machine Protection at FERMI@Elettra", Proceedings of DIPAC11, Hamburg, Germany, p. 286 (2011)
- [13] VMEbus International Trade Association, American National Standards Institute, Inc., "American National Standard for FPGA Mezzanine Card (FMC) Standard", ANSI Standard ANSI/VITA 57.1-2008, (2008), <http://www.vita.com/>